# Equilibrium Dynamics of a Polymer Bicontinuous Microemulsion

**Kristin L. Brinker,[†] Simon G. J. Mochrie,[‡] and Wesley R. Burghardt*[,§]**

*Department of Chemical and Biological Engineering, Northwestern University, Evanston, Illinois 60208; Department of Physics, Yale University, New Haven, Connecticut 06520; and Department of Chemical and Biological Engineering and Department of Materials Science and Engineering, Northwestern University, Evanston, Illinois 60208*

*Received February 26, 2007; Revised Manuscript Received May 8, 2007*

ABSTRACT: The equilibrium dynamics of a bicontinuous microemulsion composed of polystyrene, polyisoprene, and poly(styrene-*block*-isoprene) was characterized using rheology and X-ray photon correlation spectroscopy (XPCS). XPCS measurements, which probed dynamics at length scales comparable to the microemulsion domain size, show stretched-exponential relaxation of the dynamic structure factor and a wavevector-dependent Onsager coefficient. Values of the Onsager coefficient corresponding to zero wavevector ($q = 0$) and the peak of the static structure factor ($q = q_{max}$) were independently used to test rheological predictions for bicontinuous microemulsions developed by Pätzold and Dawson. The theory, which is based on a Landau−Ginzburg model, describes the shape of the relaxation spectrum and predicts the temperature dependence of the rheological properties quite well. However, for either case of the Onsager coefficient (at $q = 0$ and $q = q_{max}$), the theory fails to predict the *absolute* values of the zero-shear viscosity and average relaxation time of the microemulsion. The results of this study highlight a need for the development of more sophisticated theory to describe the rheology of bicontinuous microemulsions.

## Introduction

Over the past few decades, significant effort has been directed toward understanding the behavior of self-assembling fluids.[1−24] These fluids exhibit diverse and complex dynamics that are highly dependent on the system thermodynamics (i.e., composition and the resulting microstructure) and the dynamics of the constituent molecules. Interest in the structure and dynamics of bicontinuous microemulsions, in particular, originates from oil/water/surfactant (o/w/s) systems, which have many current industrial and biological applications.[25,26] These systems, which typically have a 10−100 nm length scale, are characterized by intertwining continuous phases of oil and water that are stabilized by a surfactant-rich interface. Recently, many studies have focused on polymer bicontinuous microemulsion (B$\mu$E) systems composed of two immiscible homopolymers (A and B) and the corresponding block copolymer (A-*b*-B).[16,19,21,24,27−37] Because of their nanoscale bicontinuous structure, polymer B$\mu$Es also possess significant potential for a variety of applications, such as optical or conductive materials, catalyst supports, and membranes.[38−41] Additionally, owing to the long chain polymer molecules, polymer bicontinuous microemulsions exhibit much slower dynamics than o/w/s systems and, thus, may serve as model systems for studying the dynamics of the B$\mu$E morphology.

**Theoretical Background.** Much of the development of theoretical descriptions for the static and dynamic behavior of bicontinuous microemulsions, to date, is based on the phenomenological Landau−Ginzburg free energy expansion $F$ of the scalar order parameter $\phi$.[4,6,10,12,13,15,42]

$$F(\phi) = a_0 + a_1\phi + a_2\phi^2 + ... + c_1(\nabla\phi)^2 + c_2(\nabla^2\phi)^2 + ... \quad (1)$$

In this case, $\phi$ represents the local deviation from the average concentration of component A or B. Teubner and Strey found that only three terms of the free energy expansion are required to describe the static structure factor, $S(q)$, of B$\mu$E systems:[42]

$$S(q) = \frac{kT}{a_2 + c_1q^2 + c_2q^4} \quad (2)$$

where $q$ [$= |\vec{q}| = (4\pi/\lambda) \sin\theta$] is the wavevector, $\lambda$ is the wavelength, $2\theta$ is the scattering angle, $k$ is the Boltzmann constant, and $T$ is temperature. Coefficients $a_2$ and $c_2$ are positive values describing fluctuations in the average composition and curvature elasticity of the interface, respectively. For B$\mu$Es, $c_1$ is negative, which drives the system to form interfaces. As the temperature is increased, $c_1$ becomes positive, and the system enters a more usual disordered phase.

Using a Landau−Ginzburg free energy description, several groups have developed expressions for the dynamics of bicontinuous microemulsions in thermal equilibrium.[4,6,10,15] Some of these analyses include a second-order parameter, $\rho$, to account for the local amphiphile concentration. The simplest case uses a Langevin equation that neglects (1) the presence of amphiphile and (2) coupling of the hydrodynamic flow field to $\phi$.[6] This description predicts single-exponential relaxation of the normalized intermediate scattering function (ISF), $f(q,t)$:

$$f(q,t) = \frac{S(q,t)}{S(q)} = \exp[-t/\tau_q] \quad (3)$$

where $\tau_q$ is the $q$-dependent relaxation time. The dynamic structure factor, $S(\vec{q},t)$, is the autocorrelation function of $\phi$ (i.e., $\langle\phi(\vec{q},t)\ \phi(-\vec{q},0)\rangle$) and, therefore, describes the rise and decay of concentration fluctuations of component A (or B) in the microemulsion.

* To whom correspondence should be addressed.
[†] Department of Chemical and Biological Engineering, Northwestern University.
[‡] Department of Physics, Yale University.
[§] Department of Chemical and Biological Engineering and Department of Materials Science and Engineering, Northwestern University.

10.1021/ma0704820 CCC: $37.00 
Published on Web 06/13/2007

More sophisticated analyses of B$\mu$E equilibrium dynamics include coupling between the order parameters ($\phi$ and $\rho$) as well as coupling of the hydrodynamic flow field to the order parameters. Using a mean-field theory approach, Granek and Cates account for these coupling relationships in their treatment of a time-dependent Landau−Ginzburg model for sponge phases.[4] In this case, their analysis for a symmetric sponge with a conserved order parameter, $\phi$, may also apply to bicontinuous microemulsions.[18] The predicted ISF is a complicated, nonexponential expression and is, therefore, excluded from this paper for brevity. Hennes and Gompper treat the same time-dependent Landau−Ginzburg model used by Granek and Cates with a field-theoretic perturbation approach; the resulting ISF decays as $f(q,t) = t^{-5/2}\exp(-t/\tau_q)$.[10] Nonomura and Ohta evaluate B$\mu$E dynamics by applying a general Brownian motion theory to derive equations of motion for $\phi$, $\rho$, and the velocity field.[15] This treatment is limited to the small $q$ range and predicts single-exponential relaxation of the ISF (eq 3). Zilman and Granek have derived expressions for membrane dynamics that are *not* based on a Landau−Ginzburg model.[11] Rather, the Helfrich bending free energy is used to describe undulations of noninteracting membrane plaquettes. This description is only valid for large $q$ and predicts stretched-exponential relaxation of the ISF: $f(q,t) = \exp[-(t/\tau_q)^{2/3}]$. The ISF expressions resulting from the more sophisticated theories indicate that relaxation in bicontinuous microemulsions occurs due to multiple processes. In general, these processes are predicted to be diffusive ($\tau_q \sim q^{-2}$) at small $q$ and nondiffusive at large $q$ with $\tau_q \sim q^{-3}$.

Pätzold and Dawson have also considered the dynamics of bicontinuous microemulsions.[12,13] Using a time-dependent Landau−Ginzburg model and subjecting the system to simple viscometric shear flow, they derived predictions for the linear viscoelastic properties. As in the Teubner−Strey model, Pätzold and Dawson write a free energy expansion using only a single order parameter, allowing for compositional variations but precluding more explicit treatment of an amphiphile that tends to locate at the interface. Their analysis also adopts the simplest possible treatment of flow effects, in which the order parameter field is advected with an imposed linear shear flow; there is no self-consistent treatment of hydrodynamics. As a result, the model is incapable of accounting for local flow modifications associated with order-parameter-dependent variation in viscosity (e.g., viscosity contrast effects) or the stresses generated by deformation of the order parameter field. Despite this simplified treatment, these rheological predictions (discussed in greater detail later in this paper) show how significant viscoelastic character results from the deformation and relaxation of the interconnected morphology in B$\mu$E systems. Implementation of the Pätzold−Dawson predictions requires knowledge of two quantities. The first is the static structure factor, which may be measured using neutron or X-ray scattering. The second quantity, the microscopic mobility (Onsager coefficient, $\Lambda$), is related to $f(q,t)$, which can be measured using photon correlation spectroscopy (PCS) techniques.

**Previous Experimental B$\mu$E Studies.** Using rheology and light photon correlation spectroscopy (LPCS), Bates, Lodge, and co-workers have characterized the equilibrium dynamics of a bicontinuous microemulsion composed of polyethylethylene (PEE), polydimethylsiloxane (PDMS), and PEE-*b*-PDMS diblock copolymer.[16,19,21] The homopolymers used in this blend were reported as Newtonian so that the B$\mu$E viscoelasticity is dominated by the blend microstructure. LPCS measurements showed that the ISF contained three exponential modes: a single dominating mode associated with collective diffusion of the B$\mu$E domains and two unidentified smaller modes that may be associated with copolymer dynamics or undulation of the interfaces.[16] The Onsager coefficient $\Lambda$ was determined from the dominant (single-exponential) B$\mu$E mode, and this information along with static scattering data was used to compute the rheological predictions of Pätzold and Dawson.[21] Although the model describes the general features of the viscoelastic behavior very well, it significantly underpredicts the magnitude of the viscosity and relaxation time of the microemulsion.

As discussed by Burghardt et al.,[21] discrepancies between experiment and the Pätzold−Dawson predictions may result from deficiencies in the model, such as its imposed linear velocity profile, which neglects any coupling between the structure and the flow field, and its inability to account for amphiphile at the interface. Burghardt et al. also noted that the Onsager coefficient may serve as a source of discrepancy. In the PEE-PDMS studies, $\Lambda$ was measured using LPCS, which probes length scales (∼500 nm) much larger than the characteristic length scale of the microemulsion (∼80 nm). However, the Onsager coefficient is expected to be $q$-dependent at smaller length scales due to hydrodynamic interactions between patches of interface.[4] Although Pätzold and Dawson do not provide any description of a $q$-dependent Onsager coefficient, perhaps the performance of the model could be improved by measuring $\Lambda(q)$ at length scales comparable to the B$\mu$E domain size.

The work by Bates, Lodge, and co-workers marks the first extensive rheological characterization of bicontinuous microemulsions as well as the first test of the rheological predictions by Pätzold and Dawson. In attempt to achieve better understanding of bicontinuous microemulsions and to provide further insight for the development of improved theories, we have characterized the equilibrium dynamics of another B$\mu$E composed of polystyrene (PS), polyisoprene (PI), and poly(styrene-*block*-iosprene) (PS-*b*-PI). In our studies, we have investigated the universality of the linear viscoelastic behavior of bicontinuous microemulsions by drawing comparisons to the previously documented PEE−PDMS B$\mu$E. Second, we have conducted X-ray photon correlation spectroscopy (XPCS) measurements to determine $f(q,t)$ and the Onsager coefficient at length scales comparable to the B$\mu$E domain size. Finally, we tested whether the use of an Onsager coefficient measured at the dominant microemulsion length scale improves the performance of the Pätzold−Dawson rheological predictions.

## Experimental Section

**Materials.** Polystyrene and polyisoprene (cis-1,4-addition), both having a molecular weight of $M_n = 3000$ and showing low polydispersity ($M_w/M_n \leq 1.08$), were obtained from Polymer Source, Inc. (Dorval, QC, Canada). Poly(styrene-*block*-isoprene), having a molecular weight of $M_n = 20\,850$ ($M_w/M_n = 1.01$) and a weight fraction of PS $w_{PS} = 0.520$, was obtained from the University of Minnesota Polymer Synthesis Facility (Minneapolis, MN). Ternary blends were prepared using equal volumes of polystyrene and polyisoprene with 5, 10, 20, 25, and 50 vol % block copolymer. Specific volumes of the polymers were determined at 160 °C using temperature-dependent expressions provided in the literature.[43] A thermal stabilizer (Irganox 1010, Ciba Specialty Chemicals) was added to the blends at 0.2 wt %, and dissolution in toluene was used to facilitate mixing of the blend components (90/10 wt % solvent/polymer). Most of the solvent was evaporated in a vacuum oven at room temperature over 8 h, and the remaining solvent was evaporated at 60 °C for 1 week. The blends were annealed for a minimum of 6−8 h at 150 °C immediately prior to experiments. The blend composed of 45/45/10 vol % PS/PI/PS-*b*-PI (total volume fraction of homopolymer, $\Phi_H = \Phi_{PS} + \Phi_{PI} = 0.90$), which exhibits a bicontinuous microemulsion phase (see

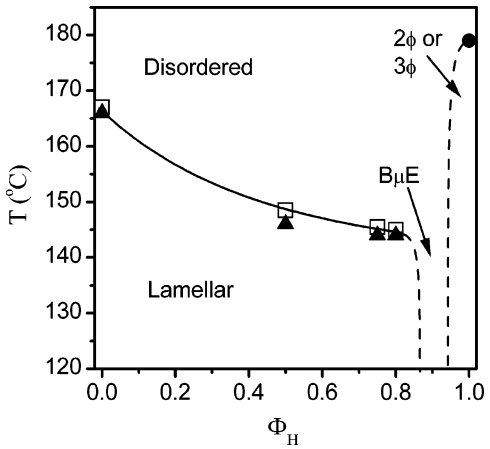


**Figure 1.** Isopleth phase diagram of PS/PI/PS-*b*-PI blends at equal volumes of PS and PI homopolymer. The abscissa represents total homopolymer concentration, $\Phi_H = \Phi_A + \Phi_B$. The order−disorder temperatures of the lamellar blends were measured by rheology (□) and birefringence (▲). The critical temperature of the binary homopolymer blend was determined via cloud point measurement (●).

Figure 1), was used in rheology, XPCS, and in-situ SAXS experiments for equilibrium studies. A fresh batch of sample was prepared for each experiment.

**Construction of the Isopleth Phase Diagram.** Birefringence measurements were performed to determine the order−disorder transition temperatures, $T_{ODT}$, of the pure diblock and of the copolymer-rich samples ($\Phi_H = 0.50, 0.75, 0.80, 0.90$). Similarly, cloud point measurements were performed to determine the critical temperature, $T_c$, of the binary homopolymer blend and of the homopolymer-rich samples ($\Phi_H = 0.90, 0.95$). These measurements were carried out using an optical microscope (Nikon OPTIPHOT2-POL) equipped with a hot stage (Mettler FP82HT). Copolymer-rich samples were heated at rate of 1 °C/min under a nitrogen atmosphere, and the disappearance of birefringence was observed as the $T_{ODT}$ was reached. Homopolymer-rich samples were cooled at a rate of 1 °C/min, and the $T_c$ was marked by a transition from translucence to turbidity of the sample.

The $T_{ODT}$'s of the copolymer-rich samples were also measured using a Rheometric Scientific ARES strain-controlled rheometer with 50 mm diameter parallel plate fixtures. Isochronal temperature scans were carried out at 5 rad/s and 0.3% strain (within the determined linear regime of the samples) with a heating rate of 0.3 °C/min. As the temperature was increased, a sharp decrease in the dynamic storage modulus was observed at the temperature at which the sample transitions from a lamellar to disordered phase.[44] The morphologies of the copolymer-rich blends were verified via SAXS measurements collected at beamline 5-ID (DND-CAT facilities) of the Advanced Photon Source (APS) at the Argonne National Laboratory. SAXS data were collected at room temperature using a 17 keV X-ray beam, 10.1 m sample-to-detector distance, and a two-dimensional MarCCD detector.

**Rheology.** Rheological measurements of the microemulsion sample ($\Phi = 0.90$) and each of the constituent homopolymers were conducted with the ARES rheometer using cone and plate fixtures (50 mm diameter, 0.04 rad cone angle). Dynamic frequency sweeps were performed in the linear regime with frequencies between 0.01 and 100 rad/s. All measurements were collected under a nitrogen atmosphere and with a temperature control of ±0.1 °C.

**X-ray Photon Correlation Spectroscopy.** XPCS experiments were performed at beamline 8-ID (IMMY/XOR-CAT facilities) of the APS using undulator radiation with a selected energy of 7.5 keV, sample-to-detector distance of 3.5 meters, and ~2 mm sample thickness. Details of XPCS setup and procedures at 8-ID are provided elsewhere.[45,46] At each measurement temperature, multiple sequences of at least 850 time-resolved scattering images were collected using a two-dimensional charge-coupled device (CCD) detector[46] and frame rates of 5, 59, and 333 Hz. For each sequence, the intensity−intensity time-autocorrelation function, $g_2(q,t)$, was computed for each pixel, where $g_2$ is defined as

$$g_2(q,t) \equiv \frac{\langle I(q,t')\, I(q,t'+t)\rangle}{\langle I(q,t')\rangle^2} \tag{4}$$

$I(q,t')$ is the scattered intensity at wavevector $q$ and time $t'$, $t$ is the delay time, and the brackets $\langle ... \rangle$ denote an average over the number of time points in the ensemble. To increase the signal-to-noise ratio, the pixels were averaged azimuthally and to a radial resolution of $\Delta q = 0.0032$ nm$^{-1}$. For each temperature and frame rate, the $g_2$ values from multiple sequences were averaged to further optimize the signal-to-noise ratio. Finally, the averaged $g_2$ values for each of the frame rates at a given temperature were merged together using a linear least-squares procedure described elsewhere.[47] XPCS measurements were collected for the PS−PI B$\mu$E at temperatures between 110 and 130 °C. For temperatures greater than 130 °C, relaxation occurs on time scales comparable to or shorter than the fast-time limit of the detector (~3 ms). Static intensity measurements were collected at several temperatures between 110 and 150 °C.

## Results and Discussion

**Phase Behavior.** The bicontinuous microemulsion used in our studies was designed using a formulation developed by Bates, Lodge, and co-workers for A/B/A−B blends, which requires that $\Phi_A = \Phi_B$, $f_A = 0.5$, $N_A \approx N_B$, and $N_{AB} \approx 5N_A$.[29] These conditions create symmetry and position the order−disorder transition of the pure block copolymer near the critical temperature of the binary homopolymer blend. $\Phi_A$ and $\Phi_B$ are the volume fractions of homopolymers A and B, respectively, and $f_A$ is the volume fraction of A in the diblock copolymer. $N_A$, $N_B$, and $N_{AB}$ are the degrees of polymerization for homopolymer A, homopolymer B, and diblock copolymer A-*b*-B, respectively. The PS/PI/PS-*b*-PI blends employed in this study yield an isopleth diagram, presented in Figure 1, that closely resembles the behavior of previously documented systems.[29,30,32,35,36] At high temperatures, all blends are disordered. At low temperatures, the copolymer-rich samples exhibit a lamellar phase, where the lamellae domains swell with increasing concentration of homopolymer. For blends near $\Phi_H \approx 0.90$ ($\Phi_H = \Phi_A + \Phi_B$), concentration fluctuations overwhelm the lamellar structure, and a bicontinuous microemulsion forms. Further increase in total homopolymer concentration results in a macrophase-separated morphology.

Birefringence and rheology measurements for the pure diblock ($\Phi_H = 0$) and copolymer-rich samples ($\Phi_H = 0.50, 0.75, 0.80$) reveal distinct order−disorder transition temperatures, which are plotted in Figure 1. Room-temperature SAXS profiles of the copolymer-rich samples show sharp, Gaussian first-order peaks[48] and smaller second- and third-order peaks, as expected for lamellar morphology (Figure 2). In symmetric lamellae, the second-order peak is suppressed, and thus, our lamellar structures appear to be slightly asymmetric. We prepared our blends such that the PS and PI domains have equal volumes at 160 °C, whereas these SAXS measurements were collected near 25 °C. Since density is a temperature-dependent quantity, the domains are anticipated to have greater symmetry at higher temperatures in the melt, where most of the experiments described in this paper were performed. As the homopolymer concentration is increased, the primary scattering peak shifts to smaller wavevectors, reflecting a swelling of the lamellar domains ($d = 2\pi/q_{max}$).

On the other side of the isopleth, the binary homopolymer blend ($\Phi_H = 1$) exhibits a distinct critical point at 179 °C in cloud point measurement. The $\Phi_H = 0.95$ sample is very turbid,

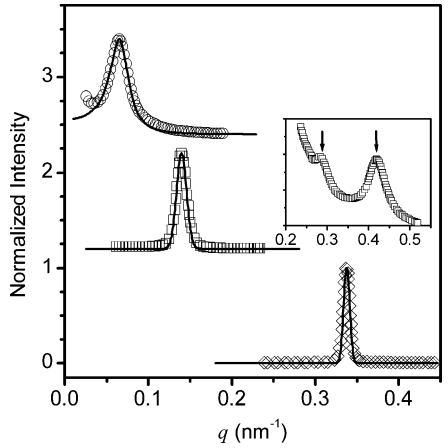


**Figure 2.** SAXS profiles of the pure diblock copolymer (◇) and ternary blends, $\Phi_H = 0.80$ (□) and $\Phi_H = 0.90$ (○), at room temperature. Gaussian curves were fit to data for the pure copolymer and $\Phi_H = 0.80$ blend, and the Teubner−Strey model (eq 2) was fit to the $\Phi_H = 0.90$ data. The fits are represented by solid lines. SAXS data are normalized by the peak intensity and shifted vertically for visual clarity. The inset features the second- and third-order peaks due to scattering from lamellar structure in the $\Phi_H = 0.80$ blend.

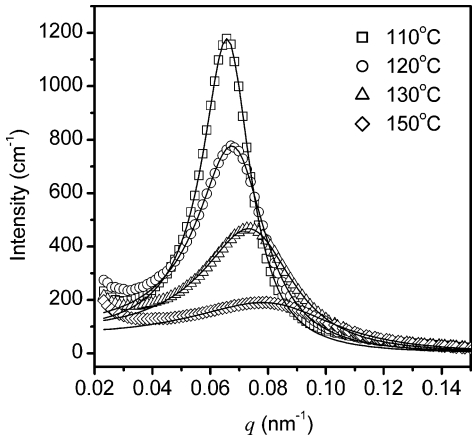


**Figure 3.** SAXS profiles of the B$\mu$E sample ($\Phi_H = 0.90$) as a function of temperature. Solid lines represent fits of the Teubner−Strey model (eq 2) to the data.

characteristic of macrophase separation, but a distinct critical point was not observed. It should be noted, however, that blends containing a small amount of block copolymer often require long equilibration times of several hours or days.[30] We did not allow for such long equilibration times in our measurements. The $\Phi_H = 0.90$ sample also exhibited some turbidity up to 195 °C, well above the critical temperature of the binary blend. This sample did not exhibit any birefringence, even at low temperatures, and a sharp drop in the storage modulus during mechanical rheometry was not observed. Therefore, neither a distinguishable order−disorder transition nor a critical point can be reported. For the $\Phi_H = 0.90$ blend, the X-ray scattering peak is much broader than the primary peaks in the copolymer-rich samples (Figure 2), and no higher order peaks are observed. In addition, the scattering peak is well-described by the Teubner−Strey structure factor (eq 2) for bicontinuous microemulsions. On the basis of these observations, we conclude the $\Phi_H = 0.90$ blend to be a bicontinuous microemulsion phase.

As shown in Figure 3, the microemulsion scattering peak persists to temperatures of at least 150 °C, beyond the disorder line of the swollen lamellar phase in the isopleth diagram. The Teubner−Strey model was fit to the scattering data collected at various temperatures, and the fitting coefficients are listed

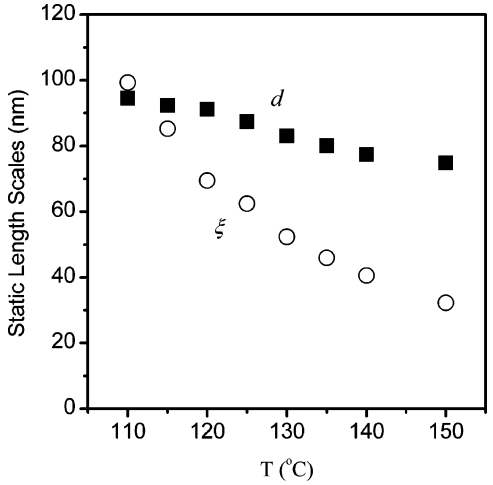


**Figure 4.** Temperature dependence of the B$\mu$E domain periodicity (■) and correlation length (○) computed from Teubner−Strey fitting coefficients.

**Table 1. Parameters from Teubner−Strey Fits to SAXS Data**

| $T$ (°C) | $q_{max}$ (nm$^{-1}$) | $a_2$ (cm) | $c_1$ (cm nm$^2$) | $c_2$ (cm nm$^4$) |
|---|---|---|---|---|
| 110 | 0.0657 | 0.00967 | −4.09 | 474 |
| 115 | 0.0671 | 0.00917 | −3.62 | 402 |
| 120 | 0.0674 | 0.00803 | −2.97 | 327 |
| 125 | 0.0701 | 0.00896 | −2.99 | 304 |
| 130 | 0.0732 | 0.00951 | −2.75 | 257 |
| 135 | 0.0754 | 0.0105 | −2.72 | 239 |
| 140 | 0.0773 | 0.0113 | −2.62 | 219 |
| 150 | 0.0780 | 0.0124 | −2.36 | 194 |

in Table 1. Some discrepancy between the microemulsion sample ($\Phi_H = 0.90$) and the model is evident at small and large wavevectors (i.e., outside the peak region). The lack of agreement at large wavevector has been reported for other B$\mu$E systems and is potentially associated with Gaussian coil scattering from the polymer chains, which predicts $I(q) \sim q^{-2}$.[29] Alternatively, local structural details in the microemulsion may not be accounted for by the Teubner−Strey model since higher order terms in the Landau−Ginzburg expansion are neglected. The discrepancy at small wavevector may result from the coexistence of larger length scale structures with the B$\mu$E phase.[28] However, the Teubner−Strey structure factor accurately represents the scattering profile in the vicinity of the peak and is, therefore, a suitable model for extracting information regarding the B$\mu$E structure from the experimental data.

The Teubner−Strey model defines two structural length scales in terms of the fitting coefficients:

$$d = 2\pi\left[\frac{1}{2}\left(\frac{a_2}{c_2}\right)^{1/2} - \frac{1}{4}\left(\frac{c_1}{c_2}\right)\right]^{-1/2} \quad (5)$$

$$\xi = \left[\frac{1}{2}\left(\frac{a_2}{c_2}\right)^{1/2} + \frac{1}{4}\left(\frac{c_1}{c_2}\right)\right]^{-1/2} \quad (6)$$

$d$ is the domain periodicity of the bicontinuous microemulsion. $\xi$ is the correlation length of the periodic structure and provides a measure of the degree of "rigidity" of the interface. The domain periodicity, plotted in Figure 4, is fairly stable within the measured temperature region, indicating stability of the microemulsion structure. The correlation length, however, decreases significantly with increasing temperature, suggesting a softening of the interface due to thermal fluctuations.[32]

For typical bicontinuous microemulsions, $\xi < d$, reflecting their lack of long-range order. As $\xi/d \rightarrow 1$ at lower temperatures

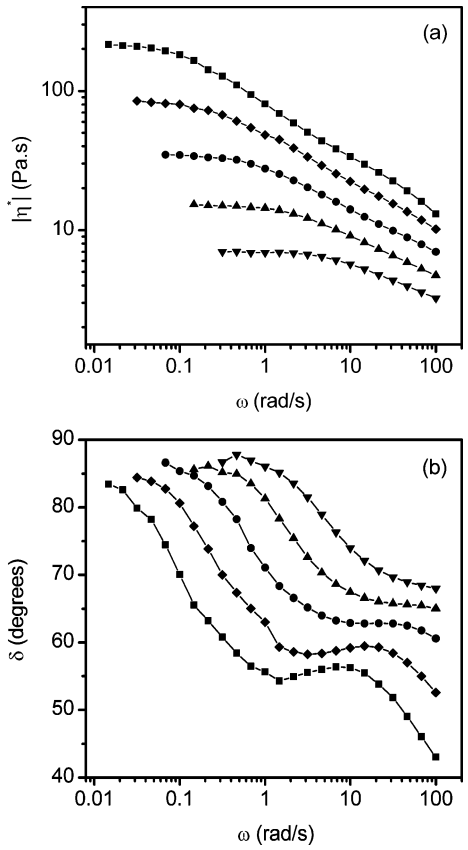


**Figure 5.** (a) Complex viscosity and (b) phase angle of the PS−PI B$\mu$E as a function of angular frequency measured at temperatures of (■) 125, (◆) 130, (●) 135, (▲) 140, and (▼) 145 °C. The solid lines serve as aids to the eye.

(near 110 °C in our sample), the microemulsion domains become more correlated. Indeed, Ryan and co-workers studied a different PS−PI B$\mu$E system for which they report $\xi/d > 1$ at sufficiently low temperatures.[37] This behavior was associated with a transition from a single-phase B$\mu$E to a biphase B$\mu$E + lamellae as the temperature was decreased. Washburn et al. also reported a transition from a single-phase B$\mu$E to a lamellar + B$\mu$E coexistence phase in a blend of poly(ethylene oxide), squalane, and poly(ethylene oxide-*b*-ethylenepropylene).[30] In the latter case, SAXS profiles support their claim of a coexistence phase; at lower temperatures, the microemulsion scattering peak is accompanied by a second prominent peak, which is associated with the coexisting lamellar structures. For our sample, the SAXS profile at 110 °C shows no evidence of additional peaks to suggest a concomitant lamellar phase. Although the trend of $\xi/d \rightarrow 1$ in Figure 4 suggests the possibility of a B$\mu$E + lamellar coexistence phase at lower temperatures, we cannot provide definitive conclusions at this time regarding the microstructure in this region. Additional measurements at these lower temperatures and for other blend compositions in or near the microemulsion channel are required.

**Rheology.** The microemulsion sample was subjected to dynamic frequency sweeps within the linear viscoelastic regime at several temperatures between 125 and 145 °C. Dynamic strain sweeps at 10 rad/s revealed the linear regime to exist for <5% strain at 125 °C and <15% strain at 145 °C. High-frequency measurements (10−100 rad/s) were conducted at lower strains (e.g., 1% strain at 125 °C, 10% strain at 145 °C). The measured complex viscosity, $|\eta^*|$, and phase angle, $\delta$, are plotted in Figure 5 as a function of angular frequency, $\omega$. At low frequencies, $|\eta^*|$ exhibits a Newtonian plateau, and $\delta \rightarrow 90°$, indicating

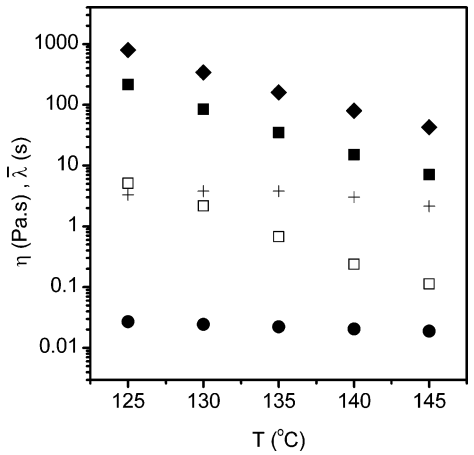


**Figure 6.** Zero-shear viscosities of the PS homopolymer (◆), PI homopolymer (●), and PS−PI B$\mu$E (■) as a function of temperature. The "background" viscosity (+) and average relaxation time of the B$\mu$E (□), determined by fitting a generalized Maxwell model to the experimental data, are also plotted.

terminal (liquidlike) behavior. At higher frequencies, $|\eta^*|$ is shear-thinning and $\delta$ decreases, which suggest perturbation of the B$\mu$E structure at these time scales. The shift in phase angle toward lower frequency with decreasing temperature is associated with a slowing down of the microemulsion dynamics. Additionally, the phase angle features a shoulder at high temperatures, which becomes a minimum followed by a downturn as the temperature decreases. The lack of self-similarity in the phase angle data indicates that the sample is not thermorheologically simple and does not obey time−temperature superposition. The increasing elasticity with decreasing temperature corresponds to an increase in the degree of segregation between the B$\mu$E domains.

Rheological measurements were also collected for each of the homopolymers. The viscosities of PS and PI, which are constant over the experimental range of frequencies, differ by more than 3 orders of magnitude (Figure 6). This large viscosity contrast reflects the large difference in glass transition temperatures of PS ($T_g \approx 82$ °C) and PI ($T_g \approx -70$ °C). The rheological data were collected closer to the glass transition of PS, and therefore, PS exhibits a stronger temperature dependence than PI. Since the molecular weights of the homopolymers are low, they are not expected to contribute significantly to the pronounced viscoelasticity of the blend shown in Figure 5. However, the polystyrene homopolymer exhibits measurable viscoelasticity at high frequencies ($\omega > 1$ rad/s) and low temperatures ($T < 135$ °C). For example, its terminal relaxation time is 0.0015 s at 125 °C. The polyisoprene homopolymer, on the other hand, does not exhibit measurable viscoelasticity within the experimental range of frequencies.

In general, the linear viscoelastic behavior of our PS−PI B$\mu$E is very similar to the PEE−PDMS B$\mu$E studied by Krishnan et al.[31] Both microemulsions are "liquidlike" at low frequency and transition to a more elastic character at higher frequency. Additionally, within the temperature ranges studied in each sample, the absolute values and temperature dependence of the zero-shear viscosities and relaxation times of the two microemulsion systems are remarkably similar. The rheological similarities are not, perhaps, entirely surprising considering the similarities in the thermodynamics (i.e., location of the B$\mu$E phase in the isopleth) as well as in the rheological properties of the constituent homopolymers. A significant difference between the two microemulsion systems is evident at the highest experimental frequencies. Following the minimum in $\delta$ at high

frequency (Figure 5b), the PS−PI system exhibits a downturn in the phase angle, thus becoming more elastic. Conversely, the PEE−PDMS system exhibits an *upturn* in the phase angle and returns to a more liquidlike state. This difference in behavior is likely related to the dynamics of the polymer chains, which may contribute to the measured viscoelasticity of the bicontinuous microemulsion at high frequencies. The homopolymers used in the PEE−PDMS microemulsion were reported to be Newtonian, whereas we report measurable viscoelasticity in our polystyrene homopolymer. Since the PS-*b*-PI copolymer is greater than 5 times the length of the homopolymers, we also expect the PS block to exhibit viscoelasticity; however, the elastic character of the PS block cannot be independently measured because the copolymer microphase separates at temperatures within the microemulsion channel. On the basis of these observations, we speculate that the elastic character of the polystyrene components in our microemulsion results in the enhanced elastic response relative to the PEE−PDMS B$\mu$E at high frequency.

The two B$\mu$E systems also show a notable difference in the "composite" zero-shear viscosity relative to the respective constituent viscosities. As shown in Figure 6, the zero-shear viscosity of the PS−PI microemulsion lies between the viscosities of the two homopolymers and exhibits a slightly stronger temperature dependence than PS due to the changing degree of segregation between the domains. If both homopolymer domains in the B$\mu$E deform equally during shear, the microemulsion viscosity should approximately equal the sum of the homopolymer viscosities weighted by the corresponding volume fractions. Using this approach, the expected viscosity of the PS−PI B$\mu$E is ∼50% of the PS homopolymer viscosity. Additional contributions from the PS−PI copolymer and its confinement to the interface could further increase the viscosity of the microemulsion. However, the zero-shear viscosity of our PS−PI microemulsion is only 17−27% of the PS viscosity. This result is in contrast to the PEE−PDMS B$\mu$E investigated by Krishnan et al., who reported the B$\mu$E zero-shear viscosity to be *larger* than the high-viscosity PEE component (which also is more than 3 orders of magnitude greater than the low-viscosity component, PDMS).[31] The lower viscosity of the PS−PI B$\mu$E (relative to the constituent viscosities) may be partially explained in terms of the degree of segregation between the domains. Structural information obtained from static scattering data show that the PS−PI microemulsion has a larger correlation length than the PEE−PDMS system. Larger correlation lengths imply an increased degree of segregation with perhaps a lesser degree of connectivity between similar domains, possibly resulting in a lower viscosity. Furthermore, the B$\mu$E viscosity may also be influenced by the degree of viscosity contrast between the homopolymers. The lower-viscosity domains deform at a greater rate than the high-viscosity domains under applied shear, yielding a lower effective "composite" viscosity. This effect may be greater in the PS−PI B$\mu$E, which has a greater viscosity contrast than the PEE−PDMS B$\mu$E.

The rheological data for the PS−PI microemulsion were fit with a generalized Maxwell model using two relaxation modes per decade. As in the PEE−PDMS B$\mu$E,[31] a purely viscous mode at zero relaxation time is necessary to accurately describe the data. This purely viscous mode is presumably dominated by the viscous dissipation of the pure components in the blend, and therefore, we refer to this viscous mode as "background" viscosity, $\eta_b$. If $\eta_b$ originates from the pure components, the temperature dependence is expected to follow that of polystyrene. For the PEE−PDMS B$\mu$E, $\eta_b$ does in fact closely follow the temperature dependence of the high-$T_g$ PEE component.[31] However, as shown in Figure 6, $\eta_b$ is insensitive to changes in temperature for the PS−PI B$\mu$E. The cause of this result is unclear and may be influenced by partial miscibility and/or high viscosity contrast between the homopolymers. Also, the microemulsion may have additional viscoelastic modes at high frequencies that are experimentally inaccessible, and the viscous contributions of these modes may be inadvertently lumped into this "background" viscosity. Estimation of $\eta_b$ solely from contributions of the homopolymers is nontrivial since their large viscosity contrast results in unequal deformation rates in the domains under applied shear; in addition, the possible role of the PS-*b*-PI copolymer cannot be estimated since the pure copolymer is microphase separated at these temperatures. Finally, estimation of $\eta_b$ in the PS−PI B$\mu$E is further complicated, relative to the PEE−PDMS microemulsion, by the elasticity of the PS components at high frequency.

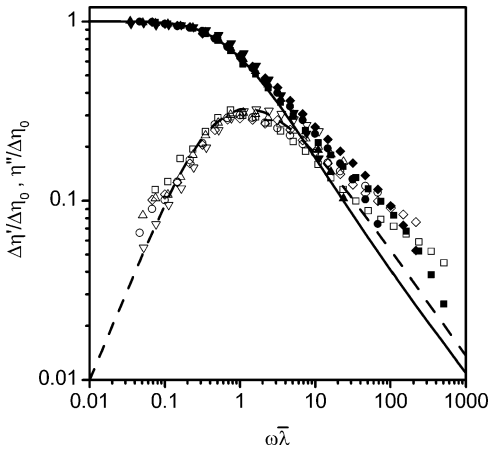


**Figure 7.** Components of the "excess" complex viscosity of the PS−PI B$\mu$E plotted in reduced form. The elastic and viscous components are represented by open and closed symbols, respectively. The solid and dashed lines are predictions based on a time-dependent Landau−Ginzburg model.[13]

Although the "background" viscosity may be an imperfect representation of the pure component contributions to the measured rheology, subtraction of $\eta_b$ from the total measured response of the B$\mu$E provides the best approximation of the "excess" viscoelasticity, resulting exclusively from the bicontinuous microstructure. Excluding the viscous "background" mode, the average relaxation time, $\bar{\lambda}$, of the microemulsion can be computed from the relaxation spectrum:

$$\bar{\lambda} = \frac{\sum \eta_k \lambda_k}{\sum \eta_k} \tag{7}$$

where $\eta_k$ and $\lambda_k$ are the viscosity and relaxation time, respectively, corresponding to each viscoelastic mode $k$ fit to the experimental data. The decrease in the average relaxation time with increasing temperature, shown in Figure 6, largely reflects an acceleration of the B$\mu$E dynamics as the constituent viscosities decrease. Also, close inspection of Figure 6 shows that $\bar{\lambda}$ exhibits a slightly stronger temperature dependence than the PS homopolymer viscosity. This enhanced temperature dependence in the relaxation time is associated with the changing degree of segregation between the homopolymer domains with temperature.

The "excess" complex viscosity components are plotted in Figure 7, where $\Delta\eta'$ ($= \eta' - \eta_b$) and $\eta''$ are the viscous and elastic components, respectively. These quantities have been normalized by the "background"-subtracted zero-shear viscosity,

$\Delta\eta_0$ ($= \eta_0 - \eta_b$), and presented as a function of the reduced frequency, $\omega\bar{\lambda}$. In this reduced form, the data collapse well into a single master curve. Some variation between data sets exists at high frequency, which may result from imperfect determination of the "background" contributions from the pure components. Despite this variation, $\Delta\eta'$ and $\eta''$ appear to merge together at high frequency.

As discussed earlier, Pätzold and Dawson have derived predictions, based on a time-dependent Landau−Ginzburg model, for the "excess" linear viscoelastic behavior of bicontinuous microemulsions.[12,13] The general predicted behavior is Rouse-like, characterized by terminal (liquidlike) response at low-frequency, changing to $\Delta\eta' \approx \eta'' \sim \omega^{-1/2}$ at high frequency. The expressions for the complex viscosity components are fairly long, so we have not included them in this paper. However, we note that the complex viscosity components in *reduced* form can be computed using structural parameters extracted from *static* X-ray or neutron scattering data. The model predictions for our PS−PI B$\mu$E, computed using SAXS data collected at 135 °C, are presented in Figure 7 along with the experimental mechanical data. (In reduced form, these predictions are only very slightly dependent on temperature over the range considered here.) As in the case of the PEE−PDMS B$\mu$E,[21] the model describes the qualitative behavior quite well with the exception at high frequency, where the predicted slope of the viscosity components (i.e., −1/2) is steeper than the experimentally observed slope. Burghardt et al. noted that the discrepancy at high frequency does not likely result from errors in lumping some of the excess properties into the viscous "background" subtraction, since increasing the viscous contribution of the B$\mu$E causes even greater deviation from the predicted behavior.[21] The PS−PI system is also complicated by possible *elastic* contributions from PS homopolymer, which enhance the measured response of the microemulsion at high frequency. Accounting for the viscoelastic contributions from polystyrene would bring the experimental data in closer agreement with theory. Despite these discrepancies, the Pätzold−Dawson model qualitatively describes the shape of the relaxation spectrum very well.

To test the ability of the Pätzold−Dawson model to predict *absolute* values of rheological parameters, measurement of the Onsager coefficient is required. We have measured the wavevector-dependent Onsager coefficient at the length scale of the microemulsion structure using XPCS. These XPCS measurements along with the quantitative performance of the model for the PS−PI B$\mu$E are discussed in the following sections of this paper.

**X-ray Photon Correlation Spectroscopy.** XPCS is a useful tool for studying the dynamics of materials, such as polymer systems, which exhibit relaxation on time scales of 0.1−100 s and length scales of 5−300 nm. Therefore, considering the static scattering and rheological results presented above, XPCS is a very suitable technique for probing the dynamics of our PS−PI microemulsion system. From XPCS measurements, the scattering intensity autocorrelation function, $g_2(q,t)$, is computed using the definition in eq 4. This quantity is related to the intermediate scattering function by

$$g_2(q,t) = 1 + A|f(q,t)|^2 \tag{8}$$

where $A$ is an experimental parameter. For a simple diffusion process, $f(q,t)$ is a single-exponential function (eq 3) with $\tau_q^{-1} = Dq^2$, where $D$ is the diffusion coefficient.

The autocorrelation function for the PS−PI B$\mu$E, shown in Figure 8 for 120 °C, does not decay as a single-exponential, indicating that the structure relaxes via multiple processes. We have chosen to fit eq 8 to our experimental data using $f(q,t)$ with a *stretched*-exponential form:

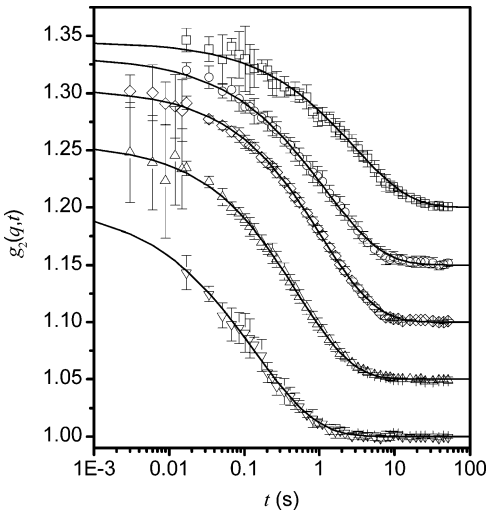


**Figure 8.** Intensity autocorrelation function as a function of delay time for the PS−PI B$\mu$E at 120 °C and various wavevectors: (□) 0.036, (○) 0.055, (◇) 0.067, (△) 0.080, and (▽) 0.09 nm$^{-1}$. For clarity, the data sets are shifted vertically from each other by 0.05. The solid lines are stretched-exponential fits.

$$f(q,t) = \exp[-(t/\tau_q)^{\nu}] \tag{9}$$

where $\nu$ is the stretching exponent. $\nu$ equals unity for single-mode relaxation and decreases as the distribution of the relaxation spectrum broadens. The average relaxation time, $\langle\tau_q\rangle$, can then be computed using the relationship[49]

$$\langle\tau_q\rangle = \left(\frac{\tau_q}{\nu}\right)\Gamma\left(\frac{1}{\nu}\right) \tag{10}$$

where $\Gamma(x)$ is the Gamma function.

The stretching exponent at higher temperatures (125 and 130 °C), as shown in Figure 9a, is nearly independent of $q$ and ranges between $0.5 \leq \nu \leq 0.65$. At lower temperatures, $\nu$ lies within this range at small $q$ but appears to become a decreasing function of $q$ for $q > q_{max}$ of the static structure factor. Furthermore, this decrease in $\nu$ at large $q$ becomes steeper with decreasing temperature. As suggested by our rheological measurements, chain dynamics appear to become significant on experimental time scales (≥10 ms) for temperatures lower than 130 °C. Therefore, at large $q$, where structures comparable to the length scale of polymer chains are probed, relaxation of the polymer chains occurs on similar time scales as microemulsion relaxation. These additional relaxation processes that are associated with chain dynamics may contribute to the broadening of the relaxation spectrum, particularly at the lowest temperatures. Although this observation complicates our interpretation of these data, it promises deeper insights into the dynamics of polymer systems.

In general, the stretching exponents determined from fits to the experimental data are close to $\nu = 2/3$ as predicted by the membrane theory by Zilman and Granek for $q \gg q_{max}$.[11] Stretched-exponential relaxation with similar values of $\nu$ have been experimentally observed in other systems containing fluctuating membranes and interfaces, including polymer vesicles[22] and o/w/s sponge phases,[50,51] lamellae,[18,20] and bicontinuous microemulsions.[17,18] Interestingly, Ruegg et al. have also recently reported stretched-exponential relaxation in a PS−PI B$\mu$E at high temperatures that transitions to *compressed*-

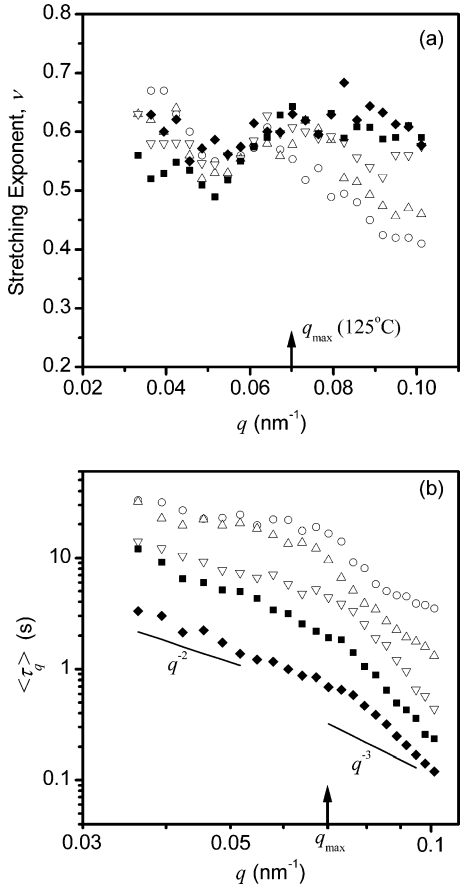


**Figure 9.** (a) Stretching exponent and (b) average relaxation time as a function of $q$ for various temperatures: (○) 110, (△) 115, (▽) 120, (■) 125, and (◆) 130 °C. The arrows indicate $q_{max}$ of the static structure factor at 125 °C.

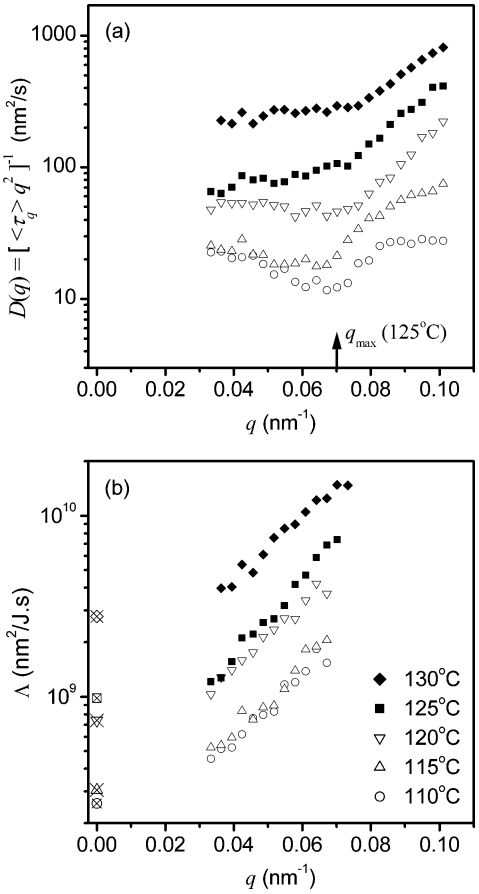


**Figure 10.** (a) $[\langle\tau_q\rangle q^2]^{-1}$ and (b) Onsager coefficient as a function of $q$ for various temperatures. Symbols with an "×" represent $\Lambda(q\rightarrow 0)$ computed using $D(q\rightarrow 0)$ from (a) and $S(q = 0)$ from eq 2.

exponential ($\nu > 1$) relaxation at low temperatures.[24] The compressed-exponential behavior, which was observed within 5−15 °C of the glass transition temperature ($T_g$) of the polystyrene homopolymer, was suggested to perhaps be related to the spontaneous breakup of microstructure. Our lowest temperature measurements are somewhat farther from the $T_g$ of the polystyrene used in the present study, and we do not observe any evidence to suggest an increase in $\nu$ or an eventual crossover to $\nu > 1$ at even lower temperatures. As indicated by the Teubner−Strey fitting coefficients, the PS−PI B$\mu$E in the present study is a more strongly structured B$\mu$E, presumably due to the larger ratio of $N_{AB}/N_A$ in our case. These differences in formulation and testing conditions may explain the differences found in these two studies.

The average relaxation time, presented in Figure 9b, decreases monotonically with increasing $q$. As the temperature decreases, however, a shoulder appears to develop in the vicinity of $q = q_{max}$ of the static structure factor, which suggests the formation of a peak at even lower temperatures. A peak in $\langle\tau_q\rangle$ occurring at $q_{max}$ of the structure factor is known as "de Gennes narrowing".[52] This behavior is often observed in systems which exhibit a peak in the structure factor resulting from a structure that is favored by low free energy. Hennes and Gompper predict a peak in $\langle\tau_q\rangle$ at $q = q_{max}$ for the condition $(2\xi/d) > 3.5$, but that $\langle\tau_q\rangle$ is a monotonically decreasing function of $q$ for $(2\xi/d) \leq 3.5$.[10] For the PS−PI B$\mu$E, $(2\xi/d) = 2.1$ at 110 °C. Therefore, the growth of the shoulder in $\langle\tau_q\rangle$ with decreasing temperature seems to be consistent with the Hennes−Gompper predictions.

For diffusive motion in systems at large length scales, the scaling relationship $\tau_q \sim q^{-2}$ is generally observed. The PS−PI B$\mu$E appears to follow this scaling for $q < q_{max}$. This behavior is perhaps more clear in a plot of $[\langle\tau_q\rangle q^2]^{-1}$ as a function of $q$, as shown in Figure 10a. For $q < q_{max}$, $[\langle\tau_q\rangle q^2]^{-1}$ is nearly independent of $q$, with the exception of the data at 110 °C. Even in the case of 110 °C, $[\langle\tau_q\rangle q^2]^{-1}$ seems to approach a constant value at the smallest measured wavevectors. For $q > q_{max}$ at all temperatures, $\langle\tau_q\rangle$ is more strongly dependent on $q$. At the highest wavevectors and lowest temperatures, however, $\langle\tau_q\rangle$ seems to return to the $q^{-2}$ scaling relationship. These observations are generally consistent with the behavior of the PS−PI B$\mu$E by Ruegg et al. for high temperatures (i.e., in the stretched-exponential regime).[24]

The Landau−Ginzburg models for bicontinuous microemulsions predict $\tau_q \sim q^{-2}$ for $q \ll q_{max}$.[4,10,15] For $q \gg q_{max}$, the Landau−Ginzburg theory by Granek and Cates predicts $\tau_q \sim q^{-3}$ as a result of hydrodynamic effects at smaller length scales.[4] The membrane theory by Zilman and Granek also predicts $\tau_q \sim q^{-3}$ for large $q$.[11] Although our experimental results agree with theoretical scaling at small $q$, the experimental relaxation time at large $q$ scales more strongly than $q^{-3}$, particularly at low temperatures. Since measurements in the high-$q$ region may be confounded by chain dynamics, it is difficult at the moment to assess this discrepancy between experiment and theory.

The Pätzold−Dawson model, which neglects the presence of amphiphile and coupling between the flow field and the order parameter, predicts single-exponential relaxation of $f(q,t)$. In the case of single-exponential relaxation where $\tau_q \sim q^{-2}$, the diffusion coefficient $D(q)$ is related to the Onsager coefficient $\Lambda$ according to

$$D(q) = [\tau_q q^2]^{-1} = \frac{kT}{S(q)}\Lambda \tag{11}$$

Although the PS−PI B$\mu$E exhibits *stretched*-exponential relaxation, we approximate the Onsager coefficient by assuming eq 11 to valid for $q \leq q_{max}$ and using the average relaxation time $\langle\tau_q\rangle$. The Onsager coefficient computed in this manner is presented in Figure 10b. In general, the Onsager coefficient increases with increasing temperature, but the strength of the temperature dependence is somewhat variable. The sample was annealed for 45 min at each temperature prior to collecting XPCS measurements. However, measurements were collected in nonsequential order with respect to temperature, and it is possible that the variability in the temperature dependence results from the sample morphology not having reached equilibrium prior to each set of measurements.

The measured Onsager coefficient is an increasing function of $q$. However, since $S(q)$ and $D(q)$ are expected to approach a constant value as $q \rightarrow 0$, $\Lambda(q\rightarrow 0)$ should also become constant. Although $D(q\rightarrow 0)$ (from Figure 10a) appears to approach a constant value at the smallest measured wavevectors, $S(q)$ (Figure 3) is still changing. To estimate $\Lambda(q\rightarrow 0)$, we have taken the experimentally determined $D(q\rightarrow 0)$ and the theoretical $S(q)$ (eq 2 using the fitting coefficients from Table 1) computed at $q = 0$. The values for $\Lambda(q\rightarrow 0)$ are plotted in Figure 10b. For $q > q_{max}$, both theory and experiment indicate that the relaxation time scales more strongly than $\tau_q \sim q^{-2}$. Since the exact scaling is unknown, we do not have an appropriate method for estimating $\Lambda(q)$ in this $q$ range. For the purpose of testing the rheological predictions by Pätzold and Dawson, we are only interested in $\Lambda(q)$ on length scales comparable to and larger than the B$\mu$E domain size ($q \leq q_{max}$).

**Landau−Ginzburg Model Predictions for Rheology.** The XPCS results above already highlight significant limitations of the single-order parameter theory underlying the analysis of bicontinuous microemulsion rheology of Pätzold and Dawson, which accounts for neither a $q$-dependent Onsager coefficient nor nonexponential relaxation of $f(q,t)$. At the same time, Figure 7 demonstrates surprisingly robust qualitative predictions of the shape of the viscoelasticity. Despite the model's shortcomings, we return here to a brief consideration of its absolute predictions of viscosity and relaxation time in order to complete the comparison with the previously studied PEE−PDMS system.[31] Pätzold and Dawson provide an expression for the "excess" zero-shear viscosity associated with the bicontinuous microstructure:

$$\Delta\eta_0 = \frac{kT\xi^3}{240\pi\Lambda c_2} f_1(\alpha) \tag{12}$$

where $\alpha = d/\xi$ and $f_1(\alpha)$ is a tabulated function defined elsewhere.[12,13] The average relaxation time of the B$\mu$E structure is given by

$$\bar{\lambda} \equiv \lim_{\omega\rightarrow 0} \frac{\eta''/\omega}{\Delta\eta'} = \frac{d^4\xi^2}{32\Lambda c_2}\frac{f_2(\alpha)}{f_1(\alpha)} \tag{13}$$

where $f_2(\alpha)$ is another tabulated function. (Expressions for $\eta''$ and $\Delta\eta'$ may be found in ref 13.) The evaluation of eqs 12 and 13 requires knowledge of structural parameters obtained from static SAXS measurements (presented in Table 1 and Figure 4) as well as the Onsager coefficient. Since Pätzold and Dawson do not account for the possibility of a $q$-dependent Onsager coefficient, we consider here only an ad hoc procedure of using

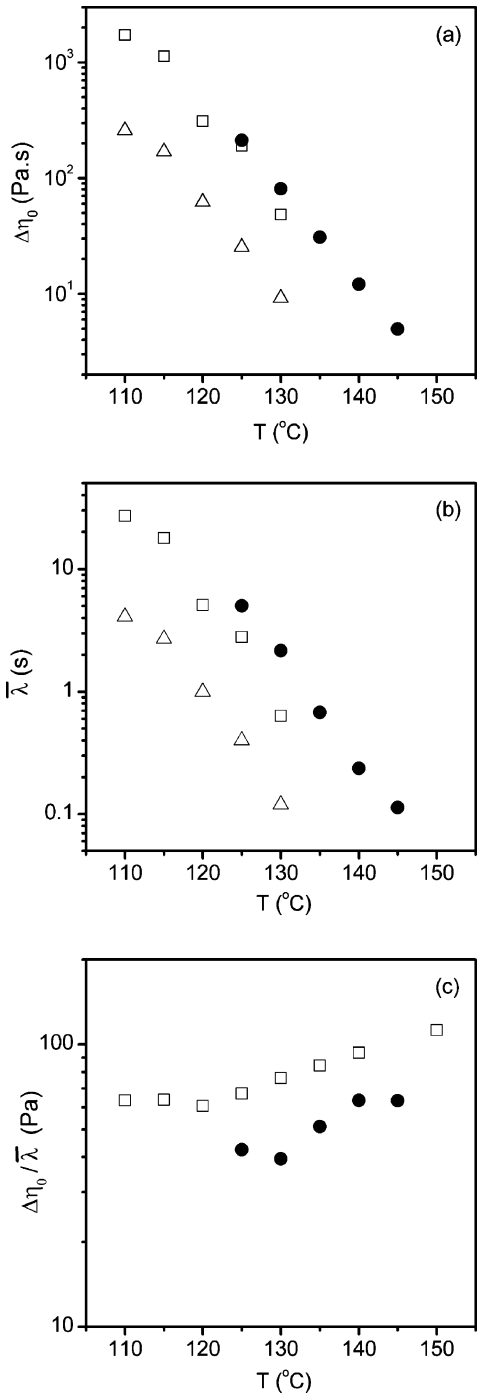


**Figure 11.** Absolute tests of the Pätzold−Dawson predictions for linear viscoelastic properties of the PS−PI B$\mu$E: (a) excess zero-shear viscosity, (b) average relaxation time, and (c) ratio of excess viscosity to relaxation time as a function of temperature. (●) Experimental data. Predictions of eqs 12 and 13 using $\Lambda(q)$ determined at (□) $q \rightarrow 0$ and (△) $q = q_{max}$ of the static structure factor.

$\Lambda(q)$ determined at $q \rightarrow 0$ and at the peak ($q = q_{max}$) of the static structure factor in evaluating the Pätzold and Dawson predictions. The former should be analogous to the use of an Onsager coefficient determined from LCPS in the PEE−PDMS study, while the latter provides a crude means of considering whether measuring dynamics on more relevant length scales impacts the quality of the predictions. The resulting two sets of predictions are plotted in Figure 11 along with the experimental data.

The model, evaluated for both cases $\Lambda(q\rightarrow 0)$ and $\Lambda(q_{max})$, underpredicts both the "excess" zero-shear viscosity and average

relaxation time. However, predictions using $\Lambda(q\rightarrow 0)$ perform significantly better than those using $\Lambda(q_{max})$. The failure of the model to predict the absolute values of the rheological properties is consistent with the study by Burghardt et al. for the PEE−PDMS B$\mu$E.[21] When using $\Lambda(q\rightarrow 0)$, the discrepancy between experiment and theory is much smaller in the PS−PI system compared to the PEE−PDMS B$\mu$E, and somewhat surprisingly, attempts to "improve" upon this by employing an Onsager coefficient measured at relevant length scales actually worsen the predictions considerably. Additionally, regardless of which Onsager coefficient is used, the predictions closely parallel the temperature dependence of the viscosity and relaxation time, which was not the case in PEE−PDMS.[31]

Burghardt et al. noted that computing the ratio $\Delta\eta_0/\bar{\lambda}$ (an effective "modulus") provides an additional quantitative test of the model. In this quantity all predicted dependence on the Onsager coefficient is removed. As shown in Figure 11c, the model fails to quantitatively predict this "modulus", which is consistent with the findings in the PEE−PDMS B$\mu$E. However, the model again performs somewhat better for the PS−PI B$\mu$E, relative to the PEE−PDMS B$\mu$E, in predicting both the absolute values and temperature dependence of $\Delta\eta_0/\bar{\lambda}$. The discrepancy between the experimental and theoretical "modulus" for the two microemulsion systems indicates that the failure of the model is related to issues other than (or in addition to) uncertainties in the measurement of $\Lambda$.

Recognizing the inherent deficiencies in the Pätzold−Dawson model revealed by the XPCS measurements of the PS−PI B$\mu$E, it is hardly surprising that its rheological predictions should fail and perhaps somewhat remarkable (or fortuitous) that it performs as well as it does in Figure 11. The results of this study underscore the need to account for more accurate physics, such as a description of hydrodynamic interactions and the presence of amphiphile, in the development of theory. Snabre and Porte[53] have performed viscosity measurements of an o/w/s sponge phase that also highlight the importance of coupling between the microstructure and the flow field in bicontinuous types of morphologies. The sponge phase exhibited Newtonian behavior over a wide range of shear rates, which suggests that the membrane is (more or less) preserved during shear. Also, the measured zero-shear viscosity as $\Phi_S \rightarrow 0$ (where $\Phi_S$ is the surfactant concentration) was much larger than the viscosity of the pure solvent. An interpretation of the results was provided indicating that the deformation of the solvent in the sponge domains (or "cells") is much greater than that of the pure solvent subjected to the same effective shear rate. As demonstrated by the Granek and Cates[4] and Hennes and Gompper[10] theories describing bicontinuous microemulsions in thermal equilibrium, accounting for hydrodynamic effects and the presence of amphiphile is nontrivial. Because of these complexities, it is difficult to speculate how the predictions of rheological properties would be impacted.

## Conclusions

The equilibrium dynamics of a polystyrene−polyisoprene bicontinuous microemulsion have been characterized using rheology and X-ray photon correlation spectroscopy. Direct comparison of the PS−PI B$\mu$E to the previously documented PEE−PDMS B$\mu$E[21,31] shows many similarities in the linear viscoelastic behavior of the two systems. Subtle differences in the overall behavior of the two microemulsions are attributed to differences in the degree of viscosity contrast and degree of segregation between the B$\mu$E domains in each system. The higher elasticity in the PS−PI B$\mu$E, relative to the PEE−PDMS B$\mu$E, at high frequency may be partially due to elastic contributions from the polystyrene components in the blend.

XPCS measurements of the PS−PI B$\mu$E show nonexponential relaxation of the intermediate scattering function and a *q*-dependent Onsager coefficient. Although the Pätzold−Dawson model predicts a *single*-exponential form of $f(q,t)$ and assumes a *q-independent* Onsager coefficient, we proceeded with an ad hoc test of its rheological predictions using $\Lambda$ determined at $q \rightarrow 0$ and $q = q_{max}$ of the static structure factor. The model generally performs better for the PS−PI B$\mu$E than for the PEE−PDMS B$\mu$E but still fails to predict the absolute values of the viscosity and average relaxation time. Furthermore, using $\Lambda$ measured at the dominant length scale of the microemulsion provides no improvement over using $\Lambda(q\rightarrow 0)$. The results of this study show the need for the development of more sophisticated theory, which account for hydrodynamic effects and the presence of amphiphile, to describe the rheological properties of bicontinuous microemulsions. And in the specific case of polymer microemulsions, the effects of the polymer chains too should be considered.

**Acknowledgment.** This work was funded by the NSF-MRSEC program (Grants DMR-0076097 and 0520513) at the Materials Research Center of Northwestern University. Funding was also provided by NSF Grant DMR-0453856. We thank Alec Sandy and Suresh Narayanan of IMMY/XOR-CAT for their help with setup of XPCS experiments at beamline 8-ID of the Advanced Photon Source, and we are grateful to Michael Sprung of IMMY/XOR-CAT for providing MATLAB programs used in computation of autocorrelation functions. We also thank Steve Weigand and the staff of DND-CAT for their help with setup of SAXS experiments at beamline 5-ID of the APS. DND-CAT is supported by the E.I. DuPont Nemours and Co., the Dow Chemical Company, and the National Science Foundation through Grant DMR-9304725 and the State of Illinois through the Department of Commerce and the Board of Higher Education Grant IBHE HECA NWU 96. The use of the Advanced Photon Source and beamlines 8-ID-I and 5-ID-D was supported by the U.S. Department of Energy, Basic Energy Sciences, Office of Research Safety, under Contract W-31-102-Eng-38.

## References and Notes

(1) Milner, S. T.; Safran, S. A. *Phys. Rev. A* **1987**, *36*, 4371−4379.
(2) Cates, M. E. *Macromolecules* **1987**, *20*, 2289−2296.
(3) Shikata, T.; Hirata, H.; Kotaka, T. *Langmuir* **1987**, *3*, 1081−1086.
(4) Granek, R.; Cates, M. E. *Phys. Rev. A* **1992**, *46*, 3319−3334.
(5) Berret, J.-F.; Roux, D. C.; Porte, G. *J. Phys. II* **1994**, *4*, 1261−1279.
(6) Gompper, G.; Hennes, M. *J. Phys. II* **1994**, *4*, 1375−1391.
(7) Farago, B.; Monkenbusch, M.; Groecking, K. D.; Richter, D.; Huang, J. S. *Physica B* **1995**, *213*, 712−717.
(8) Cates, M. E. *J. Phys.: Condens. Matter* **1996**, *8*, 9167−9176.
(9) Fredrickson, G. H.; Bates, F. S. *Annu. Rev. Mater. Sci.* **1996**, *26*, 501−550.
(10) Hennes, M.; Gompper, G. *Phys. Rev. E* **1996**, *54*, 3811−3831.
(11) Zilman, A. G.; Granek, R. *Phys. Rev. Lett.* **1996**, *77*, 4788−4791.
(12) Pätzold, G.; Dawson, K. *J. Chem. Phys.* **1996**, *104*, 5932−5941.
(13) Pätzold, G.; Dawson, K. *Phys. Rev. E* **1996**, *54*, 1669−1682.
(14) Mochrie, S. G. J.; Mayes, A. M.; Sandy, A. R.; Sutton, M.; Brauer, S.; Stephenson, G. B.; Abernathy, D. L.; Grubel, G. *Phys. Rev. Lett.* **1997**, *78*, 1275−1278.
(15) Nonomura, M.; Ohta, T. *J. Chem. Phys.* **1999**, *110*, 7516−7523.
(16) Morkved, T. L.; Chapman, B. R.; Bates, F. S.; Lodge, T. P.; Stepanek, P.; Almdal, K. *Faraday Discuss.* **1999**, *112*, 335−350.
(17) Mihailescu, M.; Monkenbusch, M.; Endo, H.; Allgaier, J.; Gompper, G.; Stellbrink, J.; Richter, D.; Jakobs, B.; Sottmann, T.; Farago, B. *J. Chem. Phys.* **2001**, *115*, 9563−9577.
(18) Komura, S.; Takeda, T.; Kawabata, Y.; Ghosh, S. K.; Hideki, S.; Nagao, M. *Phys. Rev. E* **2001**, *63*, 041402.
(19) Morkved, T. L.; Stepanek, P.; Krishnan, K.; Bates, F. S.; Lodge, T. P. *J. Chem. Phys.* **2001**, *114*, 7247−7259.

(20) Mihailescu, M.; Monkenbusch, M.; Endo, H.; Allgaier, J.; Gompper, G.; Stellbrink, J.; Richter, D.; Jakobs, B.; Sottmann, T.; Farago, B. *Appl. Phys. A: Mater. Sci. Process.* **2002**, *74*, S414−S417.
(21) Burghardt, W. R.; Krishnan, K.; Bates, F. S.; Lodge, T. P. *Macromolecules* **2002**, *35*, 4210−4215.
(22) Falus, P.; Borthwick, M. A.; Mochrie, S. G. J. *Phys. Rev. Lett.* **2005**, *94*, 016105.
(23) Falus, P.; Borthwick, M. A.; Narayanan, S.; Sandy, A. R.; Mochrie, S. G. J. *Phys. Rev. Lett.* **2006**, *97*, 066102.
(24) Ruegg, M. L.; Patel, A. J.; Narayanan, S.; Sandy, A. R.; Mochrie, S. G. J.; Watanabe, H.; Balsara, N. P. *Macromolecules* **2006**, *39*, 8822−8831.
(25) Schwuger, M.-J.; Stickdorn, K.; Schomäcker, R. *Chem. Rev.* **1995**, *95*, 849−864.
(26) Paul, B. K.; Moulik, S. P. *Curr. Sci.* **2001**, *80*, 990−1001.
(27) Bates, F. S.; Maurer, W. W.; Lipic, M. M. *Phys. Rev. Lett.* **1997**, *79*, 849−852.
(28) Lee, J. H.; Jeon, H. S.; Balsara, N. P.; Newstein, M. C. *J. Chem. Phys.* **1998**, *108*, 5173−5176.
(29) Hillmyer, M. A.; Maurer, W. W.; Lodge, T. P.; Bates, F. S.; Almdal, K. *J. Phys. Chem. B* **1999**, *103*, 4814−4824.
(30) Washburn, N. R.; Lodge, T. P.; Bates, F. S. *J. Phys. Chem. B* **2000**, *104*, 6987−6997.
(31) Krishnan, K.; Chapman, B.; Bates, F. S.; Lodge, T. P.; Almdal, K.; Burghardt, W. R. *J. Rheol.* **2002**, *46*, 529−554.
(32) Corvazier, L.; Messé, L.; Salou, C. L. O.; Young, R. N.; Fairclough, J. P. A.; Ryan, A. J. *J. Mater. Chem.* **2001**, *11*, 2864−2874.
(33) Caputo, F. E.; Burghardt, W. R. *Phys. Rev. E* **2002**, *66*, 041401.
(34) Lee, J. H.; Ruegg, M. L.; Balsara, N. P.; Zhu, Y.; Gido, S. P.; Krishnamoorti, R.; Kim, M.-H. *Macromolecules* **2003**, *36*, 6537−6548.
(35) Pipich, V.; Schwahn, D.; Willner, L. *Physica B, Suppl. 1* **2004**, *350*, E897−E900.
(36) Zhou, N.; Lodge, T. P.; Bates, F. S. *J. Phys. Chem. B* **2006**, *110*, 3979−3989.
(37) Messé, L.; Corvazier, L.; Ryan, A. J. *Polymer* **2003**, *44*, 7397−7403.
(38) Zhou, N.; Bates, F. S.; Lodge, T. P. *Nano Lett.* **2006**, *6*, 2354−2357.
(39) Gan, L. M.; Liu, J.; Poon, L. P.; Chew, C. H.; Gan, L. H. *Polymer* **1997**, *38*, 5339−5345.
(40) Wang, L.-S.; Chow, P.-Y.; Phan, T.-T.; Lim, I. J.; Yang, Y.-Y. *Adv. Funct. Mater.* **2006**, *16*, 1171−1178.
(41) Gan, L. H.; Chow, P. Y.; Liu, Z.; Han, M.; Quek, C. H. *Chem. Commun.* **2005**, *35*, 4459−4461.
(42) Teubner, M.; Strey, R. *J. Chem. Phys.* **1987**, *87*, 3195−3200.
(43) Han, C.; Kim, J.; Kim, J. K. *Macromolecules* **1989**, *22*, 383−394.
(44) Rosedale, J. H.; Bates, F. S. *Macromolecules* **1990**, *23*, 2329−2338.
(45) Sandy, A. R.; Lurio, L. B.; Mochrie, S. G. J.; Malik, G. B.; Stephenson, G. B.; Pelletier, J. F.; Sutton, M. *J. Synchrotron Radiat.* **1999**, *6*, 1174−1184.
(46) Falus, P.; Borthwick, M. A.; Mochrie, S. G. J. *Rev. Sci. Instrum.* **2004**, *75*, 4383.
(47) Lumma, D.; Lurio, L. B.; Mochrie, S. G. J.; Sutton, M. *Rev. Sci. Instrum.* **2000**, *71*, 3274.
(48) Mai, S.-M.; Fairclough, J. P. A.; Hamley, I. W.; Matsen, M. W.; Denny, R. C.; Liao, B.-X.; Booth, C.; Ryan, A. J. *Macromolecules* **1996**, *29*, 6212−6221.
(49) Lee, H.; Jamieson, A. M.; Simha, R. *Colloid Polym. Sci.* **1980**, *258*, 545−555.
(50) Freyssingeas, E.; Roux, D.; Nallet, F. *J. Phys. II* **1997**, *7*, 913−929.
(51) Maguey, M.; Bellocq, A. M. *Langmuir* **2001**, *17*, 6740−6742.
(52) de Gennes, P. G. *Physica* **1959**, *25*, 825−839.
(53) Snabre, P.; Porte, G. *Europhys. Lett.* **1990**, *13*, 641−645.

MA0704820